arXiv:0812.3586v2 [hep-ph] 23 Jan 2009

COLOR-OCTET SCALARS OF N=2 SUPERSYMMETRY AT THE LHC

S. Y. Choi[1], M. Drees[2], J. Kalinowski[3], J. M. Kim[2], E. Popenda[4] and P. M. Zerwas[4,5]

[1] *Department of Physics and RIPC, Chonbuk National University, Jeonju 561-756, Korea*
[2] *Physikalisches Inst. der Univ. Bonn, D-53115 Bonn, Germany and*
Bethe Center for Theoretical Physics, Univ. Bonn, D-53115 Bonn, Germany
[3] *Physics Department, University of Warsaw, 00681 Warsaw, Poland and*
Theory Division, CERN, CH-1211 Geneva 23, Switzerland
[4] *Inst. Theor. Physik E, RWTH Aachen U, D-52074 Aachen, Germany*
[5] *Deutsches Elektronen-Synchrotron DESY, D-22603 Hamburg, Germany and*
Laboratoire de Physique Théorique, U. Paris-Sud, F-91405 Orsay, France

(Dated: January 25, 2009)

The color gauge hyper-multiplet in N=2 supersymmetry consists of the usual N=1 gauge vector/gaugino super-multiplet, joined with a novel gaugino/scalar super-multiplet. Large cross sections are predicted for the production of pairs of the color-octet scalars σ [sgluons] at the LHC: $gg, q\bar{q} \to \sigma\sigma^*$. Single σ production is possible at one-loop level, but the $gg \to \sigma$ amplitude vanishes in the limit of degenerate L and R squarks. When kinematically allowed, σ decays predominantly into two gluinos, whose cascade decays give rise to a burst of eight or more jets together with four LSP's as signature for σ pair events at the LHC. σ can also decay into a squark-antisquark pair at tree level. At one-loop level σ decays into gluons or a $t\bar{t}$ pair are predicted, generating exciting resonance signatures in the final states. The corresponding partial widths are very roughly comparable to that for three body final states mediated by one virtual squark at tree level.

1. INTRODUCTION

The pairwise production of supersymmetric squarks and gluinos at the LHC leads to final states that contain two to four hard jets [plus somewhat softer jets from QCD radiation and/or decays of heavier neutralinos and charginos] and missing transverse momentum generated by two LSP's. These signatures are typical for N=1 supersymmetry [1, 2, 3] as specified in the Minimal Supersymmetric Standard Model [MSSM]. However, in alternative realizations of supersymmetry the final-state topology could be rather different. In order to exemplify this point, we have adopted an N=1/N=2 hybrid model, cf. Ref. [4, 5, 6], in which supersymmetry characteristics are quite different from the MSSM. Assuming the N=2 mirror (s)fermions to be very heavy in order to avoid chirality problems, the hybrid model expands to N=2 only in the gaugino sector. The QCD sector is built up by the usual N=1 gluon/gluino super-multiplet, joined with an additional gluino/scalar super-multiplet. [Similarly, the electroweak sector is supplemented by additional $SU(2)_L$ and $U(1)_Y$ super-multiplets; this sector will not be discussed here.] For the sake of simplicity we will disregard in the analysis mass splittings of the scalar fields and we assume equal masses for the usual and the novel gluinos which, as a result, can be combined to a common Dirac field, see Refs. [5, 6, 7]. Since the experimental consequences of variations involving a larger set of parameters are rather obvious, they will not be discussed in this letter.
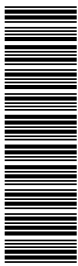
The novel scalar color-octet fields σ [which may be called scalar gluons[1], or contracted to sgluons [8]] can be produced in pairs:

$$gg,\ q\bar{q} \to \sigma\sigma^* . \tag{1.1}$$

The color-octet sgluons are R-parity even, and thus can also be produced singly in gluon-gluon or quark-antiquark collisions, albeit through loop processes only:

$$gg,\ q\bar{q} \to \sigma . \tag{1.2}$$

However, as we will show, the corresponding matrix elements vanish in the limit of degenerate L and R squarks. Moreover, single sgluon production in quark-antiquark collisions proceeds through a chirality-flip process that is suppressed, strongly in practice, by the quark mass.

At tree level, σ can decay either into (real or virtual) gluino or squark pairs,

$$\sigma \to \tilde{g}\tilde{g} \to qq\tilde{q}\tilde{q} \to qqqq + \tilde{\chi}\tilde{\chi} ,$$
$$\sigma \to \tilde{q}\tilde{q} \to qq + \tilde{\chi}\tilde{\chi} , \tag{1.3}$$

where $\tilde{\chi}$ denotes electroweak neutralinos or charginos. At one-loop level, σ can also decay into top-quark or gluon pairs:

$$\sigma \to t\bar{t} \to b\bar{b}W^+W^- ,$$
$$\sigma \to gg . \tag{1.4}$$

Apart from the last mode, these lead to spectacular signatures for σ pair production at the LHC, e.g.

$$pp \ \to\ 8\,\text{jets} + 4\,\text{LSP's} ,$$
$$pp \ \to\ tt\bar{t}\bar{t} . \tag{1.5}$$

In the first case a burst of eight almost isotropically distributed hard jets is generated in σ-pair production, even not counting QCD stray jets nor possible $\tilde{\chi}$ decay products, and a large amount of missing energy. Alternatively, four top (anti)quarks are predicted by the second mechanism. These signatures are very different from the usual MSSM topologies and raise exciting new experimental questions. Likewise, single σ production followed by gluon-pair decays generates novel resonance signatures foreign to N=1 supersymmetry.

Apart from Ref. [8], the possibility that there might exist $SU(3)_C$ octet scalars within reach of the LHC has recently been discussed in different context in Refs. [9]. While the tree-level cross sections for the pair production of these scalars at the LHC are the same in all these scenarios [up to trivial multiplicity factors], the possibilities of single production, as well as the decay modes and experimental signatures of the scalars in both channels, are quite different in our case and Ref. [8] from those discussed earlier.

This note is divided into two parts. In the next section the theoretical basis of the N=1/N=2 hybrid model will be recapitulated briefly, and the loop-induced σgg and $\sigma q\bar{q}$ couplings will be discussed. The third section is devoted to the phenomenology of σ-pair production and cascade decays, followed by a short analysis of single σ production in gluon fusion.

---

[1] Not to be confused with the scalar gluons that were discussed as carriers of the strong force in alternatives to QCD constructed in the 1970's.

2. THEORETICAL BASIS: GAUGE HYPER-MULTIPLETS AND SCALARS

As noted earlier, the N=2 QCD hyper-multiplet can be decomposed into the usual N=1 octet gluon/gluino multiplet $\hat{g} = \{g_\mu, \tilde{g}\}$ plus an N=1 octet multiplet $\hat{g}' = \{\sigma, \tilde{g}'\}$ of extra gluinos and scalar σ fields. Schematically, the QCD hyper-multiplet is described by a diamond plot,

$$
\begin{array}{ccc}
 & & \text{Spin} \\
g_\mu & & 1 \\
\tilde{g} \qquad \tilde{g}' & & 1/2 \\
\sigma & & 0
\end{array}
$$
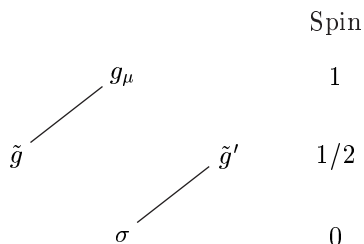
where the first, second and third row corresponds to spin 1, 1/2 and 0 states. The N=1 superfields are represented by the two pairs connected by the thin lines. The σ field carries positive R-parity.

The only gauge invariant term in the N=1 superpotential containing the new gluino/sgluon superfield $\hat{g}'$ is a mass term,

$$W_{\hat{g}'} \;=\; \frac{1}{2}\, M_3'\, \hat{g}'^a \hat{g}'^a \,, \tag{2.1}$$

where we have adopted the notation of Ref. [5]. The only supersymmetric interactions involving $\hat{g}'$ are thus QCD gauge interactions plus gauge strength $\sigma \tilde{g} \tilde{g}'$ Yukawa-type interactions [5]. In a full N=2 theory, there would also be couplings between $\hat{g}'$ and the N=2 partners of the usual matter superfields; however, in our hybrid construction we assume the latter to be decoupled from TeV scale physics.

The masses of the new scalars are determined by the superpotential (2.1) plus soft breaking terms [10]

$$\mathcal{L}_{\sigma,\,\text{soft}} = -m_\sigma^2 \left| \sigma^2 \right| - \left(m_{\sigma\sigma}^2 \sigma\sigma + \text{h.c.} \right) - g_s M_3^D \left[\sigma^a \frac{\lambda_{ij}^a}{\sqrt{2}} \sum_q (\tilde{q}_{Li}^* \tilde{q}_{Lj} - \tilde{q}_{Ri}^* \tilde{q}_{Rj}) + \text{h.c.} \right], \tag{2.2}$$

where g_s is the strong coupling constant and λ^a are the Gell-Mann $SU(3)_C$ matrices. The parameter M_3^D is the Dirac gluino mass connecting $\tilde{g}'$ with the usual gluino $\tilde{g}$ [5]. If the supersymmetry breaking is spontaneous, the Dirac gluino mass also gives rise to a supersymmetry breaking trilinear scalar interaction between σ and the MSSM squarks, as shown in Eq. (2.2); note that L and R squarks contribute with opposite signs as demanded by the general form of the super-QCD D-terms [differing from the first version of Ref. [8] with far reaching phenomenological consequences].[2] As noted above, we will set $m_{\sigma\sigma}^2 = 0$ in this discussion, so that the physical mass of the complex scalar octet is

$$M_\sigma = \sqrt{|M_3'|^2 + m_\sigma^2} \,. \tag{2.3}$$

For given mean mass, a nonzero $m_{\sigma\sigma}^2$ generating a mass splitting of the scalar fields would increase the total cross section for the production of the new scalars.

In the simplest realization the two gluinos, $\tilde{g}$ and $\tilde{g}'$, are not endowed with individual masses [i.e. $M_3' = 0$] but they are coupled by the mass parameter M_3^D in a purely off-diagonal mass matrix.[3] In this configuration the two

---

[2] If one allows oneself the freedom to break supersymmetry explicitly, but softly, the coefficients of the $\sigma \tilde{q} \tilde{q}$ interactions would be arbitrary, and could even be set to zero; this would, however, not be stable against radiative corrections.

[3] Note that this Dirac mass term must be nonzero, since otherwise the lightest member of the superfield $\hat{g}'$ would be stable. In contrast, scenarios where the diagonal Majorana entries of the gluino mass matrix vanish are perfectly acceptable.
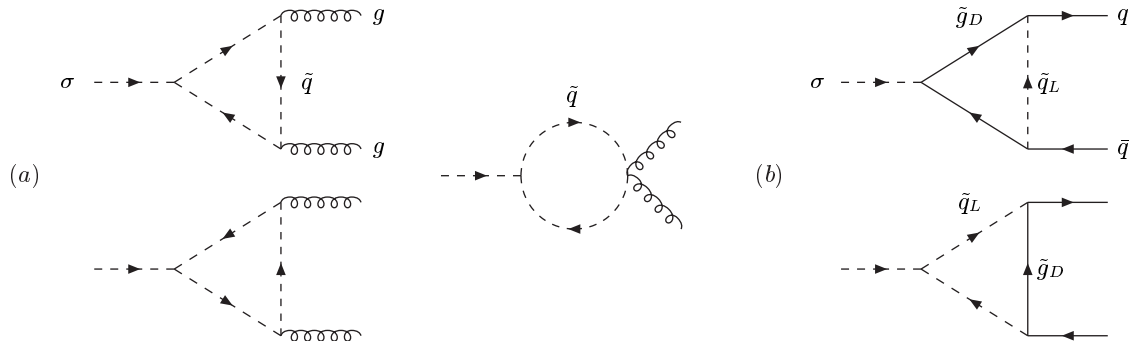
Figure 1: *Diagrams for (a) the effective σgg vertex built up by squark loops; (b) the effective $\sigma q\bar{q}$ vertex with L squarks and gluinos – the coupling to R squarks being mediated by the charge-conjugate Dirac gluinos.*

Majorana gluinos can be combined to a 4-component Dirac gluino field $\tilde{g}_D$ as

$$\tilde{g}_D = \tilde{g}_R + \tilde{g}'_L\,, \tag{2.4}$$

with the mass eigenvalue given by $|M_3^D|$, cf. Ref. [5]. The couplings of this Dirac field $\tilde{g}_D$ to the σ-field and to the squark and quark fields are summarized in the interaction Lagrangians

$$\mathcal{L}_{\tilde{g}_D\,\tilde{g}_D\,\sigma} \;=\; -\sqrt{2}i\,g_s\,f^{abc}\,\overline{\tilde{g}_{DL}^a}\,\tilde{g}_{DR}^b\,\sigma^c + \text{h.c.}\,, \tag{2.5}$$

$$\mathcal{L}_{\tilde{g}_D\,q\bar{q}} \;=\; -\sqrt{2}\,g_s \sum_q \left(\overline{q_L}\frac{\lambda^a}{2}\tilde{g}_{DR}^a\,\tilde{q}_L + \overline{q_R}\frac{\lambda^{aT}}{2}\tilde{g}_{DL}^{aC}\,\tilde{q}_R \right) + \text{h.c.}\,. \tag{2.6}$$

where $\tilde{g}_D^{CT} = -(\tilde{g}'_R + \tilde{g}_L)$ is the charge-conjugate 4-component Dirac gluino [5], f^{abc} are the $\mathrm{SU}(3)_C$ structure constants and λ^a are the Gell-Mann matrices. In addition, the sgluon fields couple to gluons in tri-and quattro-linear vertices as prescribed by gauge theories for scalar octet fields, i.e. proportional to the octet self-adjoint $\mathrm{SU}(3)_C$ representation F. As a result, at tree level σ pairs can be produced in gluon collisions as well as in $q\bar{q}$ annihilation, but single production of σ's is not possible.

Even at the one-loop level, gluino loops do not contribute to the σgg coupling, due to the Bose symmetry of the gluons. The coupling is even in the 4-momenta under gluon exchange but it is odd, on the other hand, due to the antisymmetric octet matrix elements f^{abc} in color space. [Note that $\mathrm{SU}(3)_C$ singlet particles, like Higgs bosons, couple symmetrically to gluons, by contrast.] Actually, the coupling of the octet sgluon to any number of gluons is forbidden in the general softly broken N=2 pure gauge theory with two Majorana gluinos [which may or may not be combined to a single Dirac gluino] because the totally antisymmetric factor f^{abc} forces the sgluon to couple only to two *different* Majorana gluinos, while gluons always couple to *diagonal* Majorana gluino pairs.

However, σ can couple non-trivially to gluon pairs and quark-antiquark pairs through triangle diagrams involving squark lines. Characteristic examples are depicted in Fig. 1. In parallel to the interaction Lagrangian it turns out that all L- and R-squark contributions to the couplings come with opposite signs so that they cancel each other for mass degenerate squarks. In addition, the quark-antiquark coupling is suppressed by the quark mass as evident from general chirality rules.

Comment. Before discussing the phenomenological implications, let us note that the presence of new fields in the N=1/N=2 hybrid model affects the renormalization group (RG) running of gauge couplings above the weak scale; to one-loop order,

$$\frac{d\alpha_i^{-1}(Q^2)}{d\log(Q^2)} = \frac{b_i}{2\pi}\,. \tag{2.7}$$

The coefficients b_i for the non-Abelian group factors $\mathrm{SU}(N_i)$ receive in the hybrid model contributions in addition to MSSM,

$$b_i = b_i^{\mathrm{MSSM}} - \frac{2}{3}N_i - \frac{1}{3}N_i \,, \tag{2.8}$$

where the second term comes from the new Majorana fermions $\tilde{g}'$ and the third from the complex scalars σ; the running of the $\mathrm{U}(1)_Y$ coupling remains unaffected at one-loop order. As a result, gauge coupling unification and the prediction of the weak mixing angle are lost; instead, the couplings g_i and g_j meet at different points $M_{X,ij}$, all of which lie above the Planck scale. Possible solutions to this problem would be to add fields to the theory so that the new fields fall in complete GUT multiplets [11], or to allow a different normalization for $\mathrm{U}(1)_Y$ [12], or to contemplate different unification patterns [10], etc. Since in this letter we are interested in the low-energy phenomenology of the color-octet scalars, we will not delve into this subject any further.

3. PHENOMENOLOGY OF COLOR-OCTET SCALARS AT THE LHC

3.1. σ Decays

At tree level the σ particles can decay to a pair of Dirac gluinos $\tilde{g}_D$ or into a pair of squarks, with one or both of these sparticles being potentially virtual when $M_\sigma < 2M_{\tilde{g}_D}, 2m_{\tilde{q}}$. For on-shell decays and assuming pure Dirac gluinos the partial widths are

$$\begin{aligned}
\Gamma[\sigma \to \tilde{g}_D \bar{\tilde{g}}_D] &= \frac{3\alpha_s M_\sigma}{4}\beta_{\tilde{g}}\left(1 + \beta_{\tilde{g}}^2\right), \\
\Gamma[\sigma \to \tilde{q}_a \tilde{q}_a^*] &= \frac{\alpha_s}{4}\frac{|M_3^D|^2}{M_\sigma}\beta_{\tilde{q}_a} \,,
\end{aligned} \tag{3.1}$$

where $\beta_{\tilde{g},\tilde{q}_a}$ are the velocities of $\tilde{g}, \tilde{q}_a$ $(a = L, R)$. In the presence of non-trivial $\tilde{q}_L$-$\tilde{q}_R$ mixing the subscripts L, R in the second Eq.(3.1) have to be replaced by $1, 2$ labeling the mass eigenstates, and the contribution from this flavor is suppressed by a factor $\cos^2(2\theta_{\tilde{q}})$; the mixing angle is defined via the decomposition of the lighter mass eigenstate $\tilde{q}_1 = \cos\theta_{\tilde{q}}\,\tilde{q}_L + \sin\theta_{\tilde{q}}\,\tilde{q}_R$. In addition, decays into $\tilde{q}_1\tilde{q}_2^*$ and $\tilde{q}_1^*\tilde{q}_2$ are possible, with the coefficient $\sin^2(2\theta_{\tilde{q}})$ and with the velocity $\beta_{\tilde{q}_a}$ replaced by the phase-space function $\lambda^{1/2}(1, m_{\tilde{q}_1}^2/M_\sigma^2, m_{\tilde{q}_2}^2/M_\sigma^2)$. The gluinos subsequently decay to quarks and squarks, again either real or virtual, and the squarks to quarks and charginos/neutralinos tumbling eventually down to the LSP.

On the other hand, the trilinear interaction in Eq. (2.2) gives rise to an effective σgg coupling via squark loops, Fig. 1(a), leading to the partial decay width

$$\Gamma(\sigma \to gg) = \frac{5\alpha_s^3}{384\pi^2}\frac{|M_3^D|^2}{M_\sigma}\left|\sum_q \left[\tau_{\tilde{q}_L}f(\tau_{\tilde{q}_L}) - \tau_{\tilde{q}_R}f(\tau_{\tilde{q}_R})\right]\right|^2 \,, \tag{3.2}$$

with $\tau_{\tilde{q}_{L,R}} = 4m_{\tilde{q}_{L,R}}^2/M_\sigma^2$ and [13]

$$f(\tau) = \begin{cases} \left[\sin^{-1}\left(\frac{1}{\sqrt{\tau}}\right)\right]^2 & \text{for } \tau \geq 1 \,, \\ -\frac{1}{4}\left[\ln\frac{1+\sqrt{1-\tau}}{1-\sqrt{1-\tau}} - i\pi\right]^2 & \text{for } \tau < 1 \,. \end{cases} \tag{3.3}$$

In the presence of nontrivial $\tilde{q}_L$-$\tilde{q}_R$ mixing, the subscripts L, R in Eq.(3.2) again have to be replaced by $1, 2$ labeling the mass eigenstates, and the contribution from this flavor is suppressed by a factor $\cos(2\theta_{\tilde{q}})$ multiplying the term in square parentheses. Note that the σgg coupling vanishes in the limit of degenerate L and R squarks.

Furthermore, the σ field couples to quark-antiquark pairs – in principle. By standard helicity arguments, this chirality-flip coupling is suppressed however by the quark mass. For pure Dirac gluinos, the triangle diagrams, Fig. 1(b), either with two internal gluino lines and one squark line or with two internal squark lines and one gluino line again vanish for degenerate L and R squarks. The resulting partial width can be written as

$$\Gamma(\sigma \to q\bar{q}) = \frac{9\alpha_s^3}{128\pi^2} \frac{|M_3^D|^2 m_q^2}{M_\sigma} \beta_q \left[\left(M_\sigma^2 - 4m_q^2 \right) |\mathcal{I}_S|^2 + M_\sigma^2 |\mathcal{I}_P|^2 \right] . \tag{3.4}$$

The loop integrals for the effective scalar (S) and pseudoscalar (P) couplings are given by

$$\begin{aligned}
\mathcal{I}_S &= \int_0^1 dx \int_0^{1-x} dy \left\{ (1-x-y) \left(\frac{1}{C_L} - \frac{1}{C_R} \right) + \frac{1}{9}(x+y) \left(\frac{1}{D_L} - \frac{1}{D_R} \right) \right\} , \\
\mathcal{I}_P &= \int_0^1 dx \int_0^{1-x} dy \left(\frac{1}{C_L} - \frac{1}{C_R} \right) ,
\end{aligned} \tag{3.5}$$

where we have defined ($a = L, R$)

$$\begin{aligned}
C_a &= (x+y)|M_3^D|^2 + (1-x-y)m_{\tilde{q}_a}^2 - xyM_\sigma^2 - (x+y)(1-x-y)m_q^2 , \\
D_a &= (1-x-y)|M_3^D|^2 + (x+y)m_{\tilde{q}_a}^2 - xyM_\sigma^2 - (x+y)(1-x-y)m_q^2 .
\end{aligned} \tag{3.6}$$

$\mathcal{I}_{S,P}$ can also be expressed in terms of standard Passarino-Veltman functions [14], e.g. $\mathcal{I}_P = C_{0L} - C_{0R}$, with $C_{0L,R} \equiv C_0(|M_3^D|, m_{\tilde{q}_{L,R}}, |M_3^D|; m_q^2, m_q^2, M_\sigma^2)$. In the presence of nontrivial $\tilde{q}_L$-$\tilde{q}_R$ mixing, the subscripts L, R in Eq. (3.5) have to be replaced by $1, 2$ labeling the squark mass eigenstates, and the contribution from this flavor to the double integrals is suppressed by a factor $\cos(2\theta_q)$. Note that $\mathcal{I}_S = \mathcal{I}_P = 0$ if $m_{\tilde{q}_L} = m_{\tilde{q}_R}$. In the presence of $\tilde{q}_L$-$\tilde{q}_R$ mixing this cancellation is no longer exact for two non-degenerate Majorana gluinos.
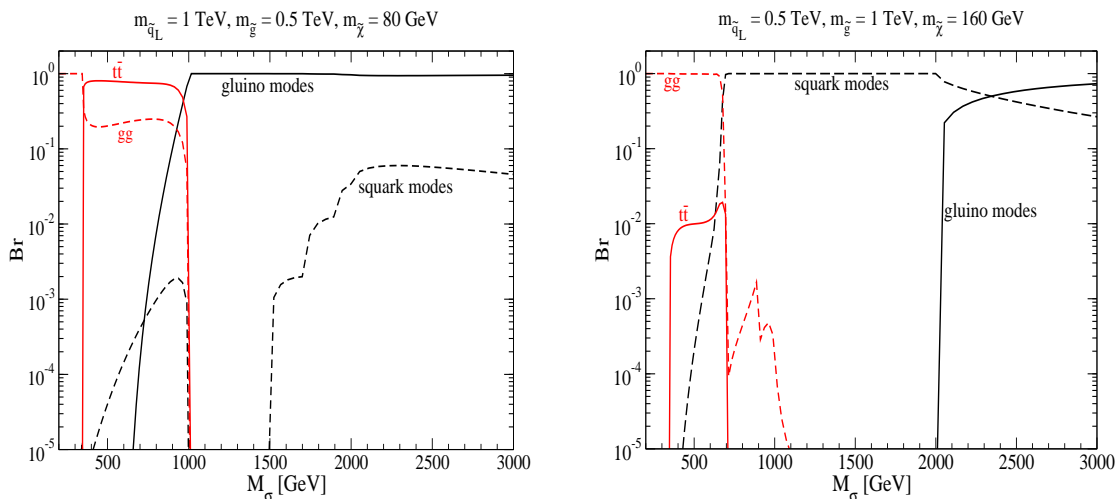
Figure 2: *Branching ratios for σ decays, for $m_{\tilde{q}_L} = 2m_{\tilde{g}} = 1$ TeV (Left) and $m_{\tilde{g}} = 2m_{\tilde{q}_L} = 1$ TeV (Right). In both cases we assumed a neutralino mass $m_{\tilde{\chi}} = 0.16 m_{\tilde{g}}$, and moderate squark mass splitting: $m_{\tilde{q}_R} = 0.95 m_{\tilde{q}_L}$, $m_{\tilde{t}_L} = 0.9 m_{\tilde{q}_L}$, $m_{\tilde{t}_R} = 0.8 m_{\tilde{q}_L}$, with $\tilde{t}_L$-$\tilde{t}_R$ mixing determined by $X_t = m_{\tilde{q}_L}$.*

The corresponding 2-body branching ratios are compared to those for tree-level decays in Fig. 2. Here we assume moderate mass splitting between the L and R squarks of the five light flavors, and somewhat greater for soft breaking $\tilde{t}$ masses: $m_{\tilde{q}_R} = 0.95 m_{\tilde{q}_L}$, $m_{\tilde{t}_L} = 0.9 m_{\tilde{q}_L}$, $m_{\tilde{t}_R} = 0.8 m_{\tilde{q}_L}$. We parameterize the off-diagonal element of the squared $\tilde{t}$ mass matrix as $X_t m_t$, and take $X_t = m_{\tilde{q}_L}$. We again assume the gluino to be a pure Dirac state, i.e. $m_{\tilde{g}} = |M_3^D|$.

Even for this small mass splitting, the loop decays into two gluons and, if kinematically allowed, a $t\bar{t}$ pair always dominate over tree-level four-body decays $\sigma \to \tilde{g}q\bar{q}\tilde{\chi}$ (which is part of the "gluino modes" in Fig. 2) and $\sigma \to q\bar{q}\tilde{\chi}\tilde{\chi}$
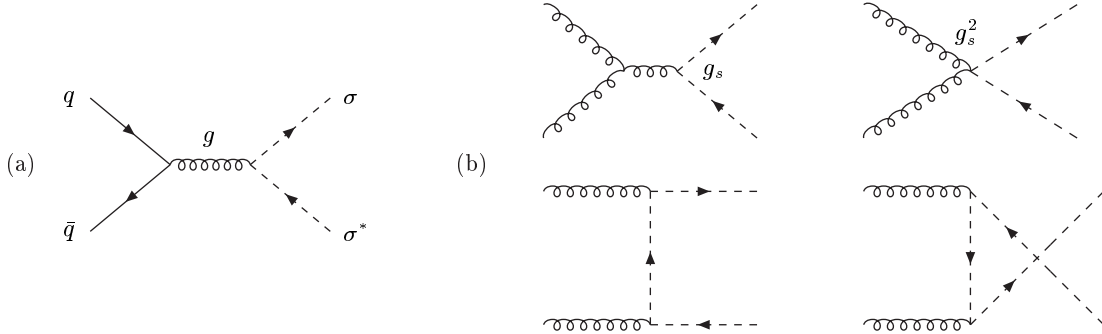
Figure 3: *Feynman diagrams for sigma-pair production in quark annihilation (a) and gluon fusion (b).*

(which is part of the "squark modes"). For simplicity we evaluated these higher order tree-level decays for a photino LSP state, with mass $0.16m_{\tilde{g}}$. $SU(2)_L$ gauginos have larger couplings to doublet squarks, but are also expected to be heavier. Including them in the final state would at best increase the partial widths for four-body final states by a factor of a few, which would still leave them well below the widths for the loop induced decays. On the other hand, the partial width for the tree-level three-body decays $\sigma \to \tilde{q}\bar{q}\tilde{\chi}$, $\tilde{q}^*q\tilde{\chi}$ can be comparable to that for the loop-induced decays if M_σ is not too much smaller than $2m_{\bar{q}}$.

Figure 2 also shows that the ordering between the two loop-induced decay modes for $M_\sigma > 2m_t$ depends on the values of various soft breaking parameters. Increasing the gluino mass increases the $\sigma\tilde{q}\tilde{q}^*$ coupling and hence the partial width into two gluons which is due to pure squark loops. On the other hand, the $t\bar{t}$ partial width, which is due to mixed squark-gluino loops, decreases rapidly with increasing gluino mass. The increase of the $\sigma\tilde{q}\tilde{q}$ couplings is over-compensated by the gluino mass dependence of the propagators. For $|M_3^D| > m_{\bar{q}}$ the loop functions $\mathcal{I}_{S,P}$ are additionally suppressed since then $C_L \simeq C_R$, $D_L \simeq D_R$ up to corrections of $\mathcal{O}(m_{\bar{q}}^2/|M_3^D|^2)$. [A similar cancellation also occurs for $M_\sigma^2 \gg m_{\bar{q}}^2$, for both the σgg and $\sigma t\bar{t}$ couplings.] In total, the $t\bar{t}$ final state will dominate for small gluino mass and the gg final state for large gluino mass. Moreover, as noted earlier, the partial width into both gluons and quarks vanishes for exact degeneracy between L and R squarks.

Not surprisingly, the two-body final states of Eq. (3.1) that are accessible at tree level will dominate if they are kinematically allowed. Note that well above all thresholds the partial width into gluinos always dominates, since it grows $\propto M_\sigma$ while the partial width into squarks asymptotically scales like $1/M_\sigma$. This is a result of the fact that the supersymmetry breaking $\sigma\tilde{q}\tilde{q}^*$ coupling has mass dimension 1, while the supersymmetric $\sigma\tilde{g}\bar{\tilde{g}}$ coupling is dimensionless.
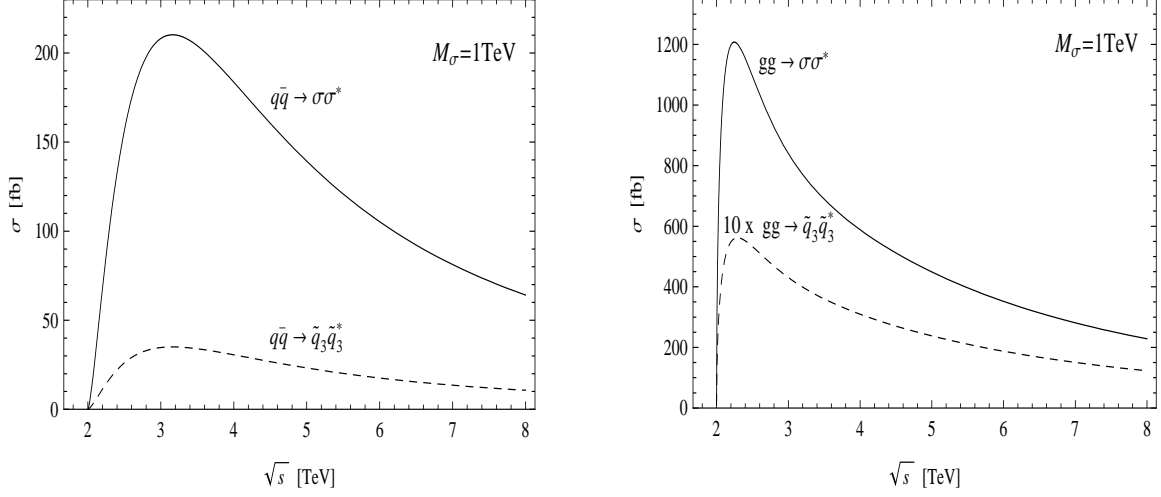
3.2. σ-Pair Production at the LHC

As summarized in the preceding section, the phenomenological analysis will be carried out for a complex color-octet σ fields without mass splitting between the real and imaginary components. The Feynman diagrams for the two parton processes $gg, q\bar{q} \to \sigma\sigma^*$ are displayed in Fig. 3. They are identical (*modulo* color factors) to squark-pair production [15, 16] if initial and final-state flavors are different.

The total cross sections for the two $\sigma\sigma^*$ parton processes are easy to calculate:

$$\sigma[q\bar{q} \to \sigma\sigma^*] = \frac{4\pi\alpha_s^2}{9s}\beta_\sigma^3\,, \tag{3.7}$$

$$\sigma[gg \to \sigma\sigma^*] = \frac{15\pi\alpha_s^2\beta_\sigma}{8s}\left[1 + \frac{34}{5}\frac{M_\sigma^2}{s} - \frac{24}{5}\left(1 - \frac{M_\sigma^2}{s}\right)\frac{M_\sigma^2}{s}\frac{1}{\beta_\sigma}\log\left(\frac{1+\beta_\sigma}{1-\beta_\sigma}\right)\right]\,. \tag{3.8}$$

Figure 4: *Parton cross sections for $\sigma\sigma^*$ production in the $q\bar{q}$ (Left) and gg (Right) channel. For comparison, the production of 3rd generation squark pairs is shown by the dashed lines for the same masses.*

The standard notation has been adopted for the parameters: $\sqrt{s}$ is the invariant parton-parton energy, and M_σ and $\beta_\sigma = (1 - 4M_\sigma^2/s)^{1/2}$ the mass and center-of-mass velocity of the σ particle. The QCD coupling is inserted to leading order, $\alpha_s(Q^2) = \alpha_s^{(5)}(Q^2)[1 + \alpha_s^{(5)}(Q^2)/(6\pi) \cdot \log M_t^2/Q^2]^{-1}$, where $\alpha_s^{(5)}(Q^2)$ evolves from $\alpha_s^{(5)}(M_Z^2) \simeq 0.120$ with $N_F = 5$ flavors by definition, while the top-quark threshold is accounted for explicitly and supersymmetric particles do not affect the running in practice; the renormalization scale for the parton subprocesses is set to $Q = M_\sigma$.

While the quark-annihilation cross section increases near threshold with the third power β_σ^3 of the sgluon velocity, as characteristic for P-wave production, the cross section for equal-helicity gluon-fusion increases steeply $\sim \beta_\sigma$ with the velocity, as predicted for S-waves by the available phase space. Asymptotically the two parton cross sections scale $\propto s^{-1}$.

The $\sigma\sigma^*$ cross sections are compared in Fig. 4 with the production of squark pairs [of the 3rd generation to match the dynamical production mechanisms]: $gg, q\bar{q} \to \tilde{q}_3\tilde{q}_3^*$. As expected, the $\sigma\sigma^*$ cross sections exceed the $\tilde{q}_3\tilde{q}_3^*$ cross sections by a large factor, i.e. ~ 20 for gg collisions and 6 for $q\bar{q}$ collisions. This can be exemplified by considering the evolution of ratios for the cross sections from small to maximum velocity, β being again the center-of-mass velocity of the sgluon or squark in the final state:

$$\frac{\sigma\left[gg \to \sigma\sigma^*\right]}{\sigma\left[gg \to \tilde{q}_3\tilde{q}_3^*\right]} = \begin{cases} \dfrac{\text{tr}\left[\{F^a, F^b\}\{F^a, F^b\}\right]}{\text{tr}\left[\left\{\frac{\lambda_a}{2}, \frac{\lambda_b}{2}\right\}\left\{\frac{\lambda_a}{2}, \frac{\lambda_b}{2}\right\}\right]} = \dfrac{216}{28/3} \simeq 23 & \text{for } \beta \to 0\,, \\[4mm] \dfrac{\text{tr}\left(2F^a F^b F^b F^a + F^a F^b F^a F^b\right)}{\text{tr}\left(2\frac{\lambda^a}{2}\frac{\lambda^b}{2}\frac{\lambda^b}{2}\frac{\lambda^a}{2} + \frac{\lambda^a}{2}\frac{\lambda^b}{2}\frac{\lambda^a}{2}\frac{\lambda^b}{2}\right)} = \dfrac{180}{10} = 18 & \text{for } \beta \to 1\,, \end{cases} \tag{3.9}$$

$$\frac{\sigma\left[q\bar{q} \to \sigma\sigma^*\right]}{\sigma\left[q\bar{q} \to \tilde{q}_3\tilde{q}_3^*\right]} = \frac{\text{tr}\left(\frac{\lambda^a}{2}\frac{\lambda^b}{2}\right)\text{tr}\left(F^a F^b\right)}{\text{tr}\left(\frac{\lambda^a}{2}\frac{\lambda^b}{2}\right)\text{tr}\left(\frac{\lambda^a}{2}\frac{\lambda^b}{2}\right)} = \frac{12}{2} = 6 \quad \text{for any } \beta\,. \tag{3.10}$$

The ratio (3.9) decreases monotonically as β increases but by no more than 20%. Most important is the ratio at the maximum of the gg cross sections where it is still close to the initial maximal value; this can easily be explained by observing that, in Feynman gauge, the leading contribution is generated by the quartic coupling. The differences in the color factors reflect the different strengths of the couplings in the fractional triplet $\lambda/2$ and the integer octet F couplings of $SU(3)_C$ with $(F^a)_{bc} = -if^{abc}$. The cross sections are shown in Fig. 4 for $M_\sigma = 1$ TeV across the invariant energy range relevant for the LHC. The values of the maxima in the gg and $q\bar{q}$ channels are about 1 pb and 0.2 pb,

respectively, a typical size for such processes.
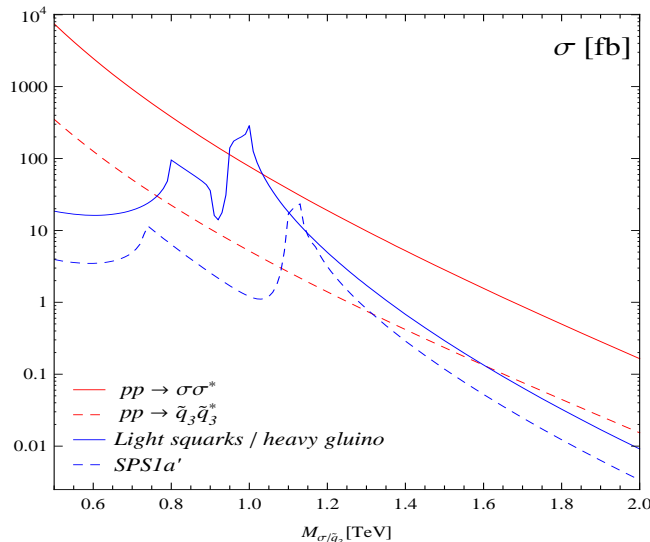
Figure 5: *Cross sections for σ-pair [and $\tilde{q}_3$-pair] production (red lines), as well as for single σ production (blue lines), at the LHC. In the latter case the solid blue curve has been obtained using the same mass parameters as in Fig.2 (Right), while the dashed blue curve adopts the mSUGRA benchmark point SPS1a'.*

The cross section for σ-pair production at LHC, $pp \to \sigma\sigma^*$, is shown by the solid red curve in Fig. 5 for the σ-mass range between 500 GeV and 2 TeV [adopting the LO CTEQ6L parton densities [17]]. The cross section exceeds stop or sbottom-pair production (red dashed line), mediated by a set of topologically equivalent Feynman diagrams, by more than an order of magnitude, as anticipated at the parton level. With values from several picobarn downwards, a sizable $\sigma\sigma^*$ event rate can be generated.

With the exception of $\sigma \to gg$ decays, all the modes shown in Fig. 2 give rise to signatures that should be easily detectable if σ is not too heavy. The most spectacular signature results from $\sigma \to \tilde{g}\tilde{g}$ decay, each σ decaying into at least four hard jets and two invisible neutralinos as LSP's. σ-pair production then generates final states with a minimum of eight jets and four LSP's, as noted in the Introduction.

The transverse momenta of the hard jets produced in the simplest case $\tilde{\chi} = \tilde{\chi}_1^0$ can easily be estimated by analyzing production and decays near the mass thresholds, i.e. $M_\sigma \simeq 2m_{\tilde{g}} \simeq 2m_{\tilde{q}} \gg m_{\tilde{\chi}_1^0}$. In this kinematic configuration the total jet transverse energy and the average jet transverse energy amount to

$$\sigma\sigma^* \ : \quad \langle E_{\perp j}^{tot} \rangle \sim 2m_{\tilde{q}} \quad \text{and} \quad \langle E_{\perp j} \rangle \sim m_{\tilde{q}}/4 \ . \tag{3.11}$$

The total transverse energy E_T carried by the LSPs and the vector sum of the momenta of the four $\tilde{\chi}_1^0$ in the final state, which determines the measured missing transverse momentum p_T, are predicted to be

$$\sigma\sigma^* \ : \quad \langle E_{\perp\tilde{\chi}}^{tot} \rangle \sim 2m_{\tilde{q}} \quad \text{and} \quad \langle p_{\perp\tilde{\chi}} \rangle \sim m_{\tilde{q}} \tag{3.12}$$

in the random-walk approximation for the $\tilde{\chi}$ momenta in the transverse plane. This is to be contrasted to gluino-pair production near threshold, where the corresponding observables are for the same mass configuration:

$$\tilde{g}\tilde{g} \ : \quad \langle E_{\perp j}^{tot} \rangle \sim m_{\tilde{q}} \quad \text{and} \quad \langle E_{\perp j} \rangle \sim m_{\tilde{q}}/4 \ , \tag{3.13}$$

$$\langle E_{\perp\tilde{\chi}}^{tot} \rangle \sim m_{\tilde{q}} \quad \text{and} \quad \langle p_{\perp\tilde{\chi}} \rangle \sim m_{\tilde{q}}/\sqrt{2} \ . \tag{3.14}$$

Thus, the total jet transverse energies and the missing transverse momenta are markedly different in the N=1 and N=2 theories for the same mass configurations.

These simple estimates are backed up by a Monte-Carlo simulation of σ-pair production at the LHC, followed by the decay into four on-shell gluinos. The total transverse jet energy and the vector sum of the LSP transverse momenta are summarized in Tab. I for a spectrum of σ-masses, and fixed ratios of gluino, squark and LSP neutralino masses. The squark and gluino masses are again chosen at about half a TeV. The values of the transverse momenta match the earlier estimates quite well. It should be noted however that the jet transverse momenta fall into two groups. The transverse momenta of jets in gluino to squark decays are generally small while the transverse momenta of the jets generated in squark decays are large. Both groups are populated equally so that the average transverse momenta of the jets are reduced by an approximate factor two compared with the MSSM gluino pair production [setting $m_{\tilde{g}}|_{\text{MSSM}} = M_\sigma|_{\text{hybrid model}}$ for the proper comparison].

Table I: *Transverse jet energies and vector sum of the LSP transverse momenta for final states in 2σ and $2\tilde{g}$ production, with primary $\sigma/\tilde{g}$-masses of 1.5 and 0.75 TeV; the mass hierarchy in the cascade decays is noted in the bottom line. Below the transverse energy per jet of the total jet ensemble [tot], the transverse energies in the high and the low jet-energy groups [high/low] are displayed. All quantities in TeV.*

$M_{\sigma/\tilde{g}}$	2σ		$2\tilde{g}$		2σ	$2\tilde{g}$
	$\langle E_{\perp j}^{tot}\rangle$	$\langle E_{\perp j}\rangle$	$\langle E_{\perp j}^{tot}\rangle$	$\langle E_{\perp j}\rangle$	$\langle p_{\perp\tilde{\chi}}\rangle$	$\langle p_{\perp\tilde{\chi}}\rangle$
1.50 TeV [tot]	1.67	0.21	1.67	0.42	0.45	0.65
[high]		0.27		0.53		
[low]		0.15		0.31		
0.75 TeV [tot]	0.91	0.11	0.93	0.23	0.22	0.31
[high]		0.14		0.29		
[low]		0.08		0.17		
$M_\sigma = 2\,M_{\tilde{g}} = 8/3\,M_{\tilde{q}} = 15\,M_{\tilde{\chi}}$						

Other interesting final states resulting from σ-pair production are four-stop states $\tilde{t}_1\tilde{t}_1\tilde{t}_1^*\tilde{t}_1^*$, which can be the dominant mode if $m_{\tilde{q}} \lesssim m_{\tilde{g}}$ and L-R mixing is significant in the stop sector, and $\tilde{q}\tilde{q}^*\tilde{g}\tilde{g}$, which can be a prominent mode if $M_\sigma > 2m_{\tilde{g}} \gtrsim 2m_{\tilde{q}}$. These channels also lead to four LSPs in the final state, plus a large number of hard jets. On the other hand, the $t\bar{t}t\bar{t}$ final state, which can be the dominant mode if the two-body decays into squarks and gluinos are kinematically excluded, might allow the direct kinematic reconstruction of M_σ.

3.3. Single σ Channel

As noted earlier, sgluons can be generated singly in gluon-gluon collisions via squark loops. The partonic cross section, with the Breit-Wigner function factorized off, is given by

$$\hat{\sigma}[gg \to \sigma] = \frac{\pi^2}{M_\sigma^3}\Gamma(\sigma \to gg)\,, \tag{3.15}$$

where the partial width for $\sigma \to gg$ decays has been given in Eq. (3.2).

The resulting cross section for single σ production at the LHC is shown by the blue curves in Fig. 5 [based on the LO CTEQ6L parton densities [17]]. The solid curve has been calculated for the parameter set of the right frame of Fig. 2, while the dashed curve has been determined by taking the soft breaking parameters in the gluino and squark sector from the widely used benchmark point SPS1a′ [18]. In the former case the single σ cross section can exceed the σ-pair production cross section for $M_\sigma \sim 1$ TeV. Since SPS1a′ has a somewhat smaller gluino mass [which we again interpret as a Dirac mass here] it generally leads to smaller cross sections for single σ production. Taking $m_{\tilde{q}} \simeq 2|M_3^D|$, as in the left frame of Fig. 2, would lead to a very small single σ production cross section. Recall that

$m_{\tilde{q}} > |M_3^D|$ is required if $\sigma \to t\bar{t}$ decays are to dominate. We thus conclude that one cannot simultaneously have a large $\sigma(pp \to \sigma)$ and a large $\mathrm{Br}(\sigma \to t\bar{t})$.

The signatures for single σ production, which is an $\mathcal{O}(\alpha_s^3)$ process, are potentially exciting as well. However, since all final states resulting from σ decay can also be produced directly in tree-level $\mathcal{O}(\alpha_s^2)$ processes at the LHC, it is a problem to be solved by experimental simulations whether single σ production is detectable as a resonance above the SM plus MSSM backgrounds, given that in most cases, with the exception of the 2-gluon channel, the direct kinematic reconstruction of M_σ is not possible.

4. SUMMARY

The color-octet scalar sector in the N=1/N=2 hybrid model we have analyzed in this letter, leads to spectacular signatures of supersymmetry which are distinctly different from the usual MSSM topologies. Depending on the masses of the particles involved, either multi-jet final states with high sphericity and large missing transverse momentum are predicted, or four top quarks should be observed in 2σ production. If the mass splitting between L and R squarks is not too small, loop-induced single σ production may also have a sizable cross section; however, this channel suffers from much larger backgrounds, though identifying the σ particle as a resonance in 2-gluon final states would truly be an exciting experimental observation.

In this letter we assumed that gluinos are pure Dirac states, and that the two components of the complex scalar field, $\sigma = (S + iP)/\sqrt{2}$, are degenerate. Relaxing these assumptions would introduce more parameters into the scheme, yet the central characteristics of the experimental event topologies of the final states at LHC would not change significantly. For example, for fixed mass, the S or P pair production cross section is simply half the σ pair production cross section.

Acknowledgments

[1] Yu.A. Golfand and E.P. Likhtman, JETP Lett. **13** (1971) 3214; J. Wess and B. Zumino, Nucl. Phys. B **70** (1974) 39.

[2] H.P. Nilles, Phys. Rept. **110** (1984) 1; H.E. Haber and G.L. Kane, Phys. Rept. **117** (1985) 75.

[3] M. Drees, R. Godbole and P. Roy, "Theory and phenomenology of sparticles: An account of four-dimensional N=1 supersymmetry in high energy physics," *Hackensack, USA: World Scientific (2004) 555 p*; P. Binetruy, "Supersymmetry:

Theory, experiment and cosmology," *Oxford, UK: Oxford Univ. Pr. (2006) 520 p*; J. Wess and J. Bagger, *Princeton, USA: Univ. Pr. (1992) 259 p*.

[4] P. Fayet, Nucl. Phys. B **113** (1976) 135; L. Álvarez-Gaumé and S.F. Hassan, Fortsch. Phys. **45** (1997) 159 [arXiv:hep-th/9701069].

[5] S.Y. Choi, M. Drees, A. Freitas and P.M. Zerwas, Phys. Rev. D **78** (2008) 095007 [arXiv:0808.2410 [hep-ph]].

[6] K. Benakli and C. Moura, *in* M. M. Nojiri *et al.*, arXiv:0802.3672 [hep-ph].

[7] M.M. Nojiri and M. Takeuchi, Phys. Rev. D **76** (2007) 015009 [arXiv:hep-ph/0701190].

[8] T. Plehn and T.M.P. Tait, arXiv:0810.3919 [hep-ph] and corrected version [*in preparation*].

[9] Z. Chacko, P.J. Fox and H. Murayama, Nucl. Phys. B **706** (2005) 53 [arXiv:hep-ph/0406142]; A.V. Manohar and M.B. Wise, Phys. Rev. D 74 (2006) 035009 [arXiv:hep-ph/0606172]; I. Antoniadis, K. Benakli, A. Delgado and M. Quiros, Adv. Stud. Theor. Phys. **2** (2008) 645 [arXiv:hep-ph/0610265]; M.I. Gresham and M.B. Wise, Phys. Rev. D **76** (2007) 075003, arXiv:0706.0909 [hep-ph]; M. Gerbush, T.J. Khoo, D.J. Phalen, A. Pierce and D. Tucker-Smith, Phys. Rev. D **77**, 095003 (2008), arXiv:0710.3133 [hep-ph]; G.L. Kane, A.A. Petrov, J. Shao and L.T. Wang, arXiv:0805.1397 [hep-ph]; M.V. Martynov and A.D. Smirnov, Mod. Phys. Lett. A **23**, 2907 (2008), arXiv:0807.4486[hep-ph]; B.K. Zur, L. Mazzucato and Y. Oz, JHEP **0810** (2008) 099, arXiv:0807.4543 [hep-ph]; P. Fileviez Perez, R. Gavin, T. McElmurry and F. Petriello, arXiv:0809.2106 [hep-ph]; C. Kilic, S. Schumann and M. Son, arXiv:0810.5542v1 [hep-ph]; C. Kim and T. Mehen, arXiv:0812.0307 [hep-ph].

[10] P.J. Fox, A.E. Nelson and N. Weiner, JHEP **0208** (2002) 035 [arXiv:hep-ph/0206096].

[11] A.E. Nelson, N. Rius, V. Sanz and M. Unsal, JHEP **0208** (2002) 039 [arXiv:hep-ph/0206102].

[12] I. Antoniadis, J.R. Ellis and G.K. Leontaris, Phys. Lett. B **399** (1997) 92 [arXiv:hep-ph/9701292]; G.D. Kribs, E. Poppitz and N. Weiner, arXiv:0712.2039 [hep-ph].

[13] J.F. Gunion and H.E. Haber, Nucl. Phys. **B278** (1986) 449.

[14] G. Passarino and M. Veltman, Nucl. Phys. **B160** (1979) 151.

[15] W. Beenakker, R. Höpker, M. Spira and P.M. Zerwas, Nucl. Phys. B **492** (1997) 51 [arXiv:hep-ph/9610490].

[16] S. Dawson, E. Eichten and C. Quigg, Phys. Rev. D **31** (1985) 1581.

[17] J. Pumplin, D.R. Stump, J. Huston, H.L. Lai, P.M. Nadolsky and W.K. Tung, JHEP **0207** (2002) 012 [arXiv:hep-ph/0201195].

[18] J.A. Aguilar-Saavedra *et al.*, Eur. Phys. J. C **46** (2006) 43 [arXiv:hep-ph/0511344].